REPORT DOCUMENTATION PAGE

Form Approved OMB No. 0704-0188

1. AGENCY USE ONLY (Leave blank)	2. REPORT DATE	3. REPORT TYPE AND DATES COVERED
	1988	Final Report

4. TITLE AND SUBTITLE

The Failure Mode of Concrete Slabs Due to Contact Charges

5. FUNDING NUMBERS

F6170893W0723

6. AUTHOR(S)

R.J.M. Van Amelsfort and J. Weerheijm

7. PERFORMING ORGANIZATION NAME(S) AND ADDRESS(ES)

Prins Maurits Laboratory
PO Box 45
2280 AA Rijswijk
The Netherlands

8. PERFORMING ORGANIZATION REPORT NUMBER

SPC-93-4043

9. SPONSORING/MONITORING AGENCY NAME(S) AND ADDRESS(ES)

EOARD
PSC 802 BOX 14
FPO 09499-0200

10. SPONSORING/MONITORING AGENCY REPORT NUMBER

SPC-93-4043

11. SUPPLEMENTARY NOTES

12a. DISTRIBUTION/AVAILABILITY STATEMENT

Approved for public release; distribution is unlimited.

12b. DISTRIBUTION CODE

A

13. ABSTRACT (Maximum 200 words)

A study of the failure of concrete slabs due to contact charges has been made. The main theoretical aspects are described and the results of an experimental program with different set-ups are given. A discussion of these data together with the conclusions drawn from them end the report..

14. SUBJECT TERMS			15. NUMBER OF PAGES 42 / 16. PRICE CODE
17. SECURITY CLASSIFICATION OF REPORT	18. SECURITY CLASSIFICATION OF THIS PAGE	19. SECURITY CLASSIFICATION OF ABSTRACT	20. LIMITATION OF ABSTRACT
UNCLASSIFIED	UNCLASSIFIED	UNCLASSIFIED	UL

prins maurits laboratorium tno

Copy prior to changes

Contract/Grant Number: Grant AFOSR-86-0340

THE FAILURE MODE OF CONCRETE SLABS DUE TO CONTACT CHARGES

R.J.M. van Amelsfort, M.Sc., J. Weerheijm, M.Sc.
Prins Maurits Laboratorium TNO
P.O.Box 45
2280 AA RIJSWIJK
The Netherlands

November 1988

Final Scientific Report, Sept. 30th, 1986 - Sept. 29th, 1988

Prepared for:

USAF, Air Force Office of Scientific Research
Bolling AFB, DC 20332 - 6448

and

European Office of Aerospace Research and Development
London, England.

SUMMARY

A study of the failure of concrete slabs due to contact charges has been made. The main theoretical aspects are described and the results of an experimental program with different set-ups are given.
A discussion of these data together with the conclusions to be drawn from them end the report.

SAMENVATTING

Een studie naar het bezwijken van betonnen platen ten gevolge van contactladingen is uitgevoerd. De belangrijkste theoretische aspecten worden beschreven en de resultaten van een experimenteel programma met verschillende opstellingen worden gegeven. Het rapport wordt afgesloten met een bespreking van deze gegevens en de hieruit te trekken conclusies.

CONTENTS

LIST OF SYMBOLS

a,b,r	dimensions of the contact charge	mm
A	square of the hole	m^2
c	longitudinal wave velocity	m/s
d	hole diameter	mm
d_b	crater diameter at the back	mm
d_c	critical thickness	mm
d_f	crater diameter at the front	mm
f_c	static compression strength	Pa
f_{cd}	dynamic compression strength	Pa
F_b^p	load due to the detonation pressure	N
h	slab thickness	mm
I_s	impulse supplied to the pendulum	kgm/s
I_s^p	total impulse as derived theoretically (Pahl)	kgm/s
I_t	impulse transmitted to the pendulum	kgm/s
I_{ta}	transmitted impulse, determined with V_a	kgm/s
I_{tf}	transmitted impulse, determined with V_f	kgm/s
I_{tp}	transmitted impulse, determined with V_p	kgm/s
I_t^a	polynomial fit value of the transmitted impulse	kgm/s
M	mass involved in the dominant force	g
P	pressure	Pa
P_b	dynamic strength	Pa
P_{g1}	mass with particle size > 1 mm diameter	%
P_{g4}	mass with particle size > 4 mm diameter	%
P_{l1}	mass with particle size < 1 mm diameter	%
P_p	load performed by the particle stream	Pa
Q	weight of the charge	g
R	radius of assumed load surface	m
t_d	pressure duration time	s
u	particle velocity	m/s
U_{max}	maximum amplitude of pendulum deflection	mm
V	average velocity of M	m/s

LIST OF SYMBOLS (continued)

V_a	velocity measured with acceleration transducers	m/s
V_f	velocity measured with film technique	m/s
V_p	velocity determined with pendulum deflection	m/s
W	weight of the contact charge	N
ρ	mass density	kg/m^3

1. INTRODUCTION

Protection of, for instance, shelters against direct hits, can be obtained with layered structures. These structures often comprise two concrete slabs with an intermediate layer of sand. The first concrete slab is the deceleration layer which has to stop a bomb or projectile. The sand layer is the pressure distribution and energy absorption layer which has to damp the shock waves, and thus prevents spalling of the protected structure. The second concrete slab is the protection layer of personnel and/or equipment behind it. Often this second slab is part of the protected structure itself. This type of layered structures has especially been developed to stop missiles and to prevent spalling at the back of the slab.

However, due to the layered composition of the construction, an undesirable phenomenon may occur when a missile explodes after it has been stopped. The current study concerns this phenomenon. In the study it is assumed that a missile just penetratres the first slab and then explodes. To simulate this situation, experiments have been performed with contact charges on concrete slabs. From earlier experiments performed at the TNO Prins Maurits Laboratorium it is known that when these types of loading exceed a certain critical value, a concentrated stream of high-velocity particles is formed, originating from the crushed concrete. These particles penetrate the intermediate layer and form a severe loading for the inner plate or protection layer. Very little is known about the origin and properties of this particle stream. The aim of this study is to gain some insight into the process of failure of the concrete slab and to gather data to quantify the loading due to the particle stream.

This report first gives a short description of some theoretical aspects of the failure mode of concrete slabs. To get information of the threat formed by the particle stream, numerical data with respect to the impulse or energy exerted by the particle stream for

instance, must be known. An experimental programme has been carried out to obtain the parameters of interest. Numerical data of the velocity, divergence and total mass of this particle stream and the particle and size distribution itself, have been determined for various charge weights. When these data are known, the threat of the particle stream can be described. When more information of the threat is known, it becomes possible to take measures for protection. In the discussion of the experimental results an attempt is made to join theory and experimental data together.

2. THE FAILURE MODE OF A CONCRETE SLAB

When a contact charge detonates, temperature and pressure increase to very high levels (of the order of 5000 to 7000 K and 10 to 20 GPa) and the concrete near the contact area melts and is completely crushed. The strength of the material is of minor importance because of the high pressure occurring in this region. The pressure wave expands in the slab and so the pressure decreases with increasing distance to the charge. With this decreasing pressure the influence of the strength of the materials involved increases. The pressure decreases until it reaches the linear elastic stress level of the slab at which the concrete can withstand the load (Weerheijm et al., 1984).

2.1 The behaviour of concrete with increasing compression

Concrete is a mixture of sand and gravel embedded in a cement matrix. The latter is the weakest link in the concrete and will crush first when the load increases. A crushing cement matrix results in a decreasing internal cohesion and an increasing deformation of the material. If the load increase is continued, the cement matrix will be fully crushed and the sand and gravel particles are loaded directly. This results in an increase in the

strength of the concrete. Further increase in the load results in crushing the particles as well. It is a generally accepted assumption that under the conditions of an instantaneously increasing pressure, concrete starts to lose its internal strength at a stress level of about 8 to 10 times the static compression strength (Pahl, 1979).

2.2 Stress waves, crater formation and spalling

An extensive description of the stress waves and the process of crater formation and spalling is given in (Weerheijm et al., 1984) A summary will be given in this section.
The pressure in the contact area of the charge and the slab is of the order of 10 to 20 GPa. This stress level together with the shape of the stress wave determine the strength of the concrete, and this strength in its turn determines the propagation velocity of the stress wave. This is shown in Figure 1, which gives the stress - strain relation of concrete for hydrostatic pressure and volumetric strain. This stress - strain relationship governs the wave velocity (c) and the profile of the pressure wave.
Immediately after the explosion a stress wave corresponding with the high stress level (10 to 20 GPa), is initiated. The pressure rapidly decreases with increasing distance from the initiation point and the lower stress level causes a different shape of the stress wave (Figure 1). Below stress level C in Figure 1 the first load of the concrete is performed by the precursor or elastic wave with a stress level of about 8 to 10 times the static compression strength. The stress level increases and the concrete is crushed behind this wave front. The velocity of expansion of the region in which the concrete is fully crushed appears to be smaller than the longitudinal wave velocity (Weerheijm et al., 1984). This means that the cratering process in a concrete slab,

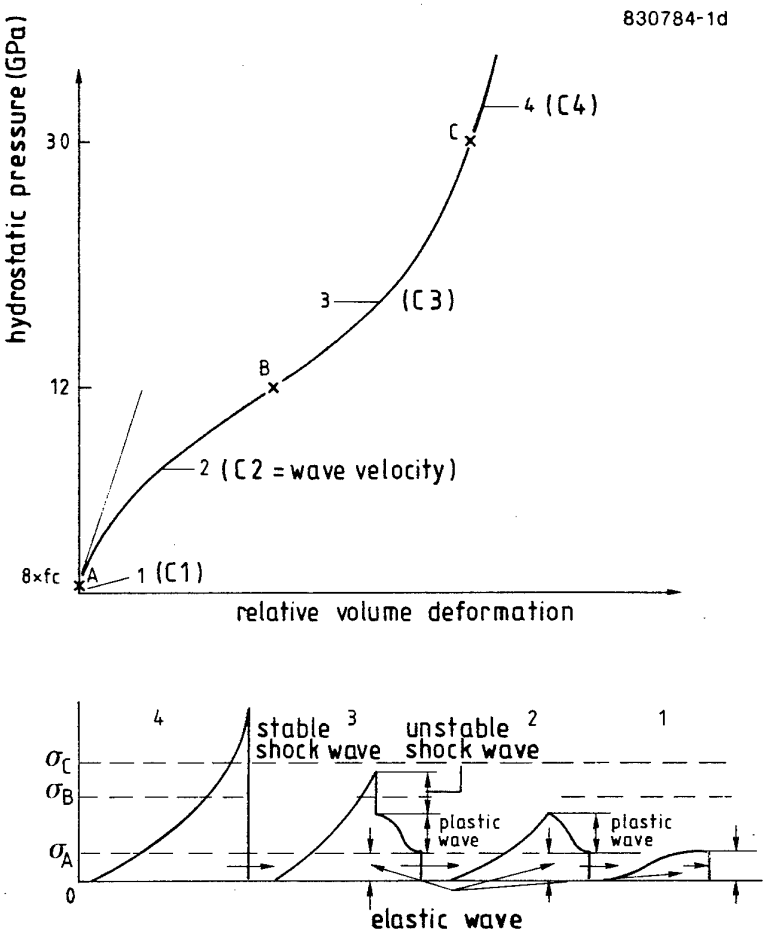

Figure 1. Relationship between pressure stresses and relative volume deformations and the variation in the profile of the pressure wave for the different regions. (Weerheijm et al., 1984).

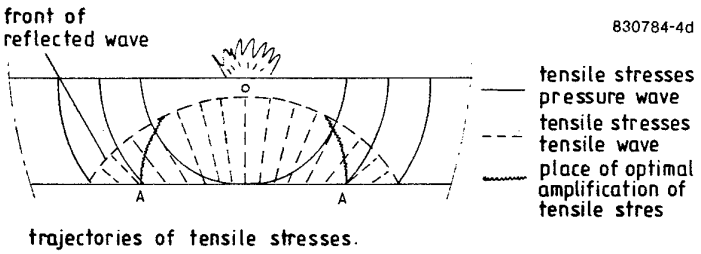

Figure 2. Trajectories of tensile stresses (Weerheijm et al., 1984).

which can only occur in the crushed zone, can be disturbed by the elastic waves reflected from the back of the slab as tensile waves. This is shown in Figure 2, which gives the trajectories of the tensile stresses. The consequences of this interference will be discussed later.

The particle velocity u due to a plane stress wave is given by the quotient of the pressure P and the acoustic impedance (product of density ρ and longitudinal wave velocity c).

$$u = \frac{P}{\rho \cdot c} \qquad (1)$$

For crushed material the particle velocity will increase due to the increasing stress and the decreasing impedance. The radial movement of the particles will be obstructed by less crushed material. When this resistance is sufficient the radial trajectories are deflected, the crushed material is ejected and a crater is formed. As mentioned earlier this cratering process can be partly disturbed by the reflected (tensile) stress waves. The interference of waves during the cratering process results in principal tensile and compression stresses. Because of the small tensile strength of concrete, spalling can occur over nearly the whole area, covered by the reflected wave. The resistance of the material in front of the crushed zone to the movement of the particles in this zone decreases continuously by the expansion of the crushing zone and by spalling and cracking at the rear of the slab. When the reflected wave reaches the crushing zone in the concrete slab the particles are ejected downwards and cratering is stopped. Owing to the high stresses in the area around the charge the energy of the concentrated particle stream can be very high. This process of forming a concentrated particle stream will occur above some critical values (Weerheijm et al., 1984). A slab will fail in this critical way when its thickness equals $13.4 * Q^{1/3}$ mm, where Q is the weight of the charge in grams.

3. PROBLEM DEFINITION

In the previous section a theoretical explanation is given of the origin of a concrete particle stream when a concrete slab is loaded with a contact charge greater than a critical charge. Also the lack of knowledge of the properties of this particle stream has been mentioned. From previous experiments a severe loading has been observed. To quantify the loading and to enlarge the knowledge about the process, the experimental programme focussed on mass, velocity, divergence and particle size distribution of the particle stream. Different experimental set-ups have been developed to measure the different parameters. An experimental technique with optical fibres embedded in the concrete (Appendix) has been developed to determine the parameters of the concrete itself. When these parameters are known, quantities such as the impulse or energy of the particle stream can be calculated. When the total impulse of the particle stream is known, the force that may be exerted by the stream on following layers, can be estimated. Table 1 gives a review of all experiments performed, together with the purpose of each experiment.
The results of the experiments 01 up to and including 010 and 1 up to and including 25 have already been given and discussed in the progress reports (Amelsfort and Weerheijm, 1987).

4. EXPERIMENTAL RESULTS

All experiments have been performed with 60-mm-thick concrete slabs with the following characteristics:

- laboratory quality B22.5
- maximum diameter of the river gravel/sand 8 mm.
- reinforcement Feb 500 HWL $\varnothing$ 8 mm
- mesh width upper reinforcement 100 mm

- mesh width lower reinforcement 75 mm
- covering below and above the reinforcement 5 mm
- compressive strength 25 to 30 N/mm^2
- specific mass 2200 kg/m^3.

Review of all experiments performed. Table 1.

Experiment number	Type of experiment	Purpose is measurement of:
01,02,03	vertical	mass, particle size distribution
04 through 08	horizontal	particle stream velocity, impulse
09,010	vertical	particle stream velocity, divergence
1 through 4	vertical	critical velocity
5 through 12	vertical	critical velocity (two slabs)
13 through 18	vertical	mass, particle size distribution
19 through 25	horizontal	impulse
26 through 42	vertical	particle stream velocity, divergence
43 through 64	horizontal	impulse

The thickness of 60 mm has been chosen to perform experiments on plates of the same thickness as performed earlier with the layered structures. Another more practical reason concerns the weight and handling of the specimens.

Two types of experiments have been performed. A vertical set-up is used to measure masses and particle sizes and to film the particle stream. A horizontal set-up is used to measure the load (impulse) exerted by the particle stream. The identifications horizontal and vertical refer to the direction of the particle stream as can be seen in Figures 3 and 4 which give a view of both set-ups. A more

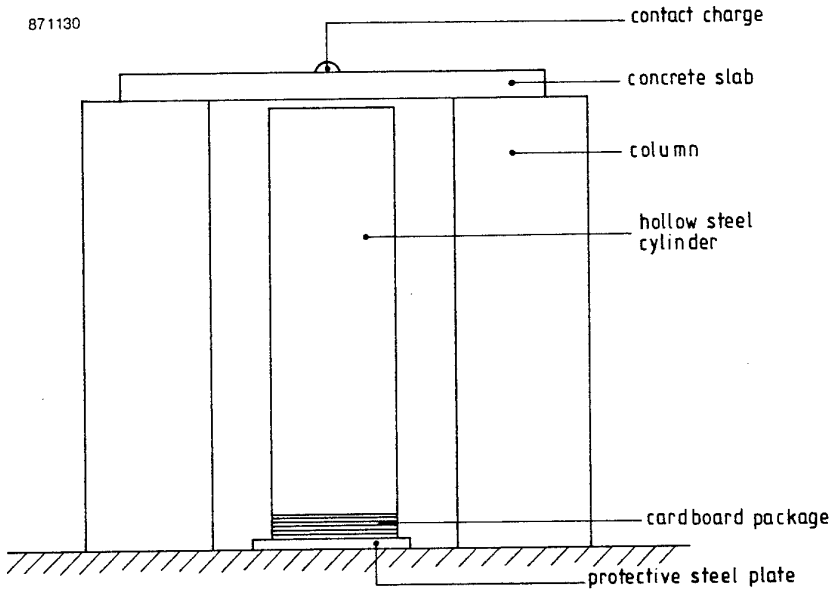

Figure 3. Front-view of vertical experimental set-up.

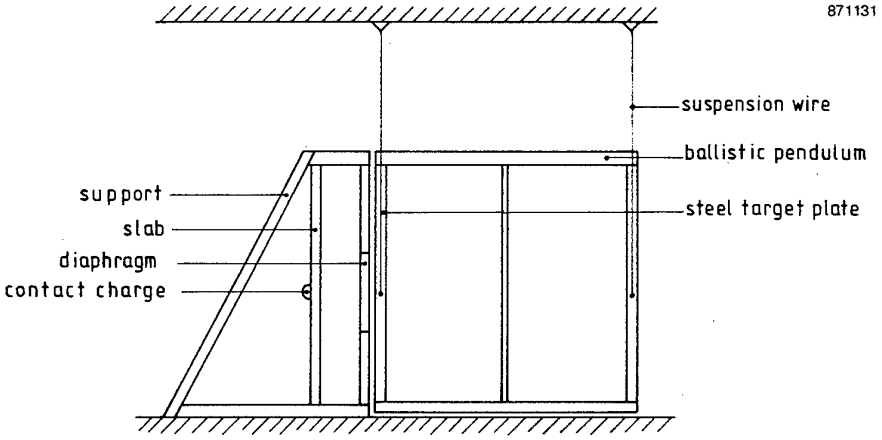

Figure 4. Side-view of horizontal experimental set-up.

detailed description of both set-ups is given in (Amelsfort and Weerheijm, 1987).

All experiments were performed with hemispherical contact charges of high explosives with 80 % penthrite and 20 % inert material.

4.1 Determination of the critical value

The results of the experiments in the vertical set-up with two concrete slabs on top of each other, supported at four corners and loaded in the centre of the top slab are given in Table 2 (Amelsfort and Weerheijm, 1987).

Results of the experiments performed to obtain the critical value for the contact charge Table 2.

Charge (g)	Experiment number	Result (experiments with two slabs)
70	7	both slabs not perforated
80	6	first slab perforated, second slab not
	8	both slabs not perforated
85	10	first slab perforated, second slab not
	11	first slab perforated, second slab not
90	5	both slabs perforated
	12	both slabs perforated

From Table 2 it can be concluded that the critical charge for 60 mm thick concrete slabs is about 85 g PETN (80 %). The formula given in (Weerheijm et al., 1984):

$$d_c = 13.4 * Q^{1/3} \qquad (2)$$

where d_c is the critical thickness (mm) and Q is the weight of the charge (g), yields for Q = 85 g a value for the thickness of d_c = 58.9 mm. This is in good agreement with the observed critical thickness for a charge weight of 85 to 90 grams used in the experiments (60 mm).

4.2 Determination of the crater dimensions

A summary of all experimental results, as well in the horizontal as in the vertical set-up, concerning the crater and hole dimensions is given in Table 3. The symbols used are defined in Fig.5.

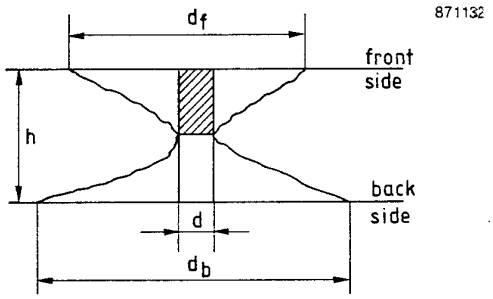

Figure 5. Crater and hole dimensions in a concrete slab loaded with a contact charge.

These data can be fitted by an exponential function. If the charge Q is set in grams, these functions are:

crater diameter at the front side: $d_f = 58.7 * Q^{0.3}$ (mm) (3)

hole diameter : $d = 30.9 * Q^{0.36}$ (mm) (4)

crater diameter at the back side : $d_b = 78.3 * Q^{0.3}$ (mm) (5)

With a few exceptions these formulae result in crater dimensions within 10% of the measured values. Table 4 shows a review of the average values and the calculated values of the crater dimensions. Figure 6 gives photographs of the craters on both sides of the slab after the shot. Crater and hole profiles can be seen clearly.

Review of the crater and hole dimensions measured after each experiment

Table 3.

Charge (g)	Crater dimensions (mm) d_f	d	d_b	Experiment numbers
20	140	60	180	4
40	160	120	250	3
50	2*160 180 6*190 2*200 2*210	120 10*130 3*140	190 2*200 220 230 240 2*250 2*260 270 2*280	2,22,26,28 31,34,39,43 44,49,52,53 58,59
70	3*210 2*220 230	5*140 150	270 280 2*300 330	17,18,20,23 35,40
75	-	140	290	1
85	190 200 4*220 7*230 2*240 250	7*150 7*160 170 180	250 270 3*280 290 3*300 2*310 320 3*330	13,16,19,24 27,29,32,36 41,45,46,50 54,55,60,61
120-125	210 4*230 240 2*250 2*260	140 150 2*160 5*170 180	270 4*280 4*290 310	01,02,03,04 05,06,07,08 09,010
170	250 4*260 6*270 2*280 3*290	180 4*190 7*200 3*210 220	4*320 330 3*340 2*350 3*360 370	14,15,21,25 30,33,37,38 47,48,51,56 57,62,63,64

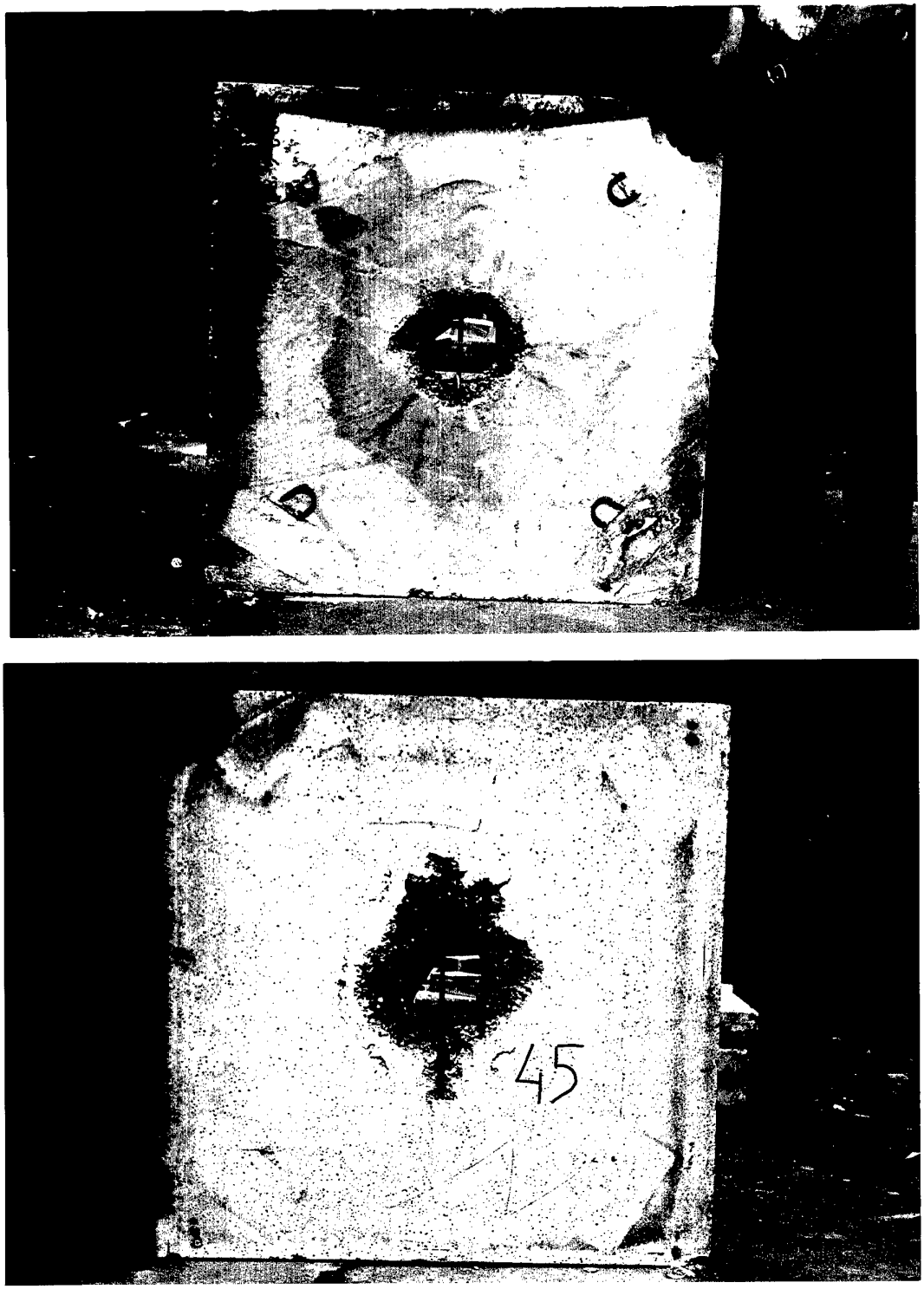

Figure 6. Crater formation at the front (photo above) and at the back (photo below) of the concrete slab. (Charge 85 g)

Average and calculated values of the crater dimensions

Table 4.

Charge (g)	Crater dimensions (mm) front (d_f) average	front (d_f) calc.	hole (d) average	hole (d) calc.	back (d_b) average	back (d_b) calc.	number of exp.
20	140	144	60	91	180	192	1
40	160	177	120	116	250	237	1
50	189	190	131	126	241	253	14
70	217	210	142	142	296	280	6
75	-	214	140	146	290	286	1
85	225	222	157	153	299	297	16
125	239	250	164	175	286	333	10
170	271	274	199	196	341	365	16

4.3 Determination of the impulse of the particle stream

In order to get some idea of the magnitude of the impulse of the particle stream several experiments were performed with both the horizontal and the vertical set-up (Amelsfort and Weerheijm, 1987). With a ballistic pendulum method (Kolkert and Amelsfort, 1982 and 1983) the impulse transferred to the pendulum by the particle stream can be derived. The particle stream hits a target plate fixed in the ballistic pendulum and gives the pendulum an initial velocity and a maximum amplitude. This initial velocity of the pendulum has been meausured/calculated in three ways:

- By filming the movement of the pendulum the initial velocity (V_f) of the pendulum is determined.
- By integrating the signals of acceleration transducers fixed on the pendulum (Amelsfort and Weerheijm, 1987) the initial velocity (V_a) of the pendulum is determined. The acceleration signals are subjected to some treatments before and after the

integration, such as filtering, offset and drift correction. These treatments do not affect the amplitude of the acceleration and velocity signals.

- By measuring the maximum magnitude (U_{max}) of the deflection of the pendulum the initial velocity (V_p) of the pendulum is calculated, as described in (Amelsfort and Weerheijm, 1987).

The results of all three methods are depicted in Table 5. Please note the two different weights of the pendulums and the three different distances between the back of the loaded concrete slab and the front of the target plate fixed in the pendulum:

Types of pendulum:

a. weight 245.5 kg, pendulum length 0.975 m and period 1.8 s, distance between concrete slab and target plate 1.05 m.

b. weight 519.0 kg, pendulum length 1.01 m and period 1.875 s, distance between concrete slab and target plate 0.245 m.

c. weight 519.0 kg, pendulum length 1.01 m and period 1.875 s, distance between concrete slab and target plate 0.557 m.

Figure 7 shows the heavy weight pendulum at the left. The concrete slab with the load is situated at the right of the photo. Figure 8 is an example of the integrated signals of the acceleration transducers.

Multiplication of the results obtained for the initial pendulum velocity and the weight of the pendulum yields the impulse (I_t) transmitted to the pendulum. Table 6 gives these results for the impulse transmitted to the pendulum by the concrete particle stream. The subscript f in I_{tf} indicates that the initial velocity of the pendulum has been measured with the film technique, the subscript a in I_{ta} indicates that the initial velocity of the pendulum has been measured with the acceleration transducer technique, and the subscript p in I_{tp} indicates that the initial velocity of the pendulum has been calculated from the measured maximum deflection of the pendulum. The mass of the concrete particles on the target plate in the pendulum can be neglected with regard to the pendulum weight.

Experimentally obtained initial velocities of the ballistic pendulum loaded by a concrete particle stream. Table 5.

Charge (g)	Exp. no.	V_f (m/s)	V_a (m/s)	V_p (m/s)	U_{max} (mm)	Type of pendulum
50	22	.19	.10-.17	.22	70	a
	43	.17	.11-.12	-	-	b
	44	.09	.07-.08	-	-	b
	49	.11	.06-.07	.13	41	c
	52	.10	.09-.12	.11	37	b
	53	.10	.07-.10	.10	34	b
	58	.08	.06-.08	.10	31	c
	59	.10	.06-.07	.10	33	c
70	20	.42	.31-.32	.37	117	a
	23	.29	.36-.38	.34	108	a
85	19	.45	.42-.44	.47	149	a
	24	.46	.47-.48	.45	143	a
	45	.19	.16-.20	-	-	b
	46	-	.19-.22	-	-	b
	50	.16	.10-.12	.14	45	c
	54	.22	.21-.25	.19	63	b
	55	.20	.22-.26	.19	63	b
	60	.24	.14-.17	.19	61	c
	61	.24	.12-.15	.20	64	c
170	21	.91	.74-.85	.83	261	a
	25	.70	.78-.78	.79	251	a
	47	.37	.41-.45	-	-	b
	48	.40	.42-.44	.36	115	b
	51	.28	.22-.27	-	-	c
	56	.41	.40-.45	.34	108	b
	57	.42	.46-.49	.36	115	b
	62	.38	-	.41	132	c
	63	.38	.38-.43	.35	113	c
	64	.39	.36-.40	.38	121	c

From the results of Table 6 it can be concluded that the order of magnitude for the impulse I_t transmitted to the pendulum amounts to about 50 kgm/s for the 50 g load, about 110 kgm/s for the 85 g load and about 220 kgm/s for the 170 g load. At least for the first part of the trajectory (about 1 m), the impulse transmitted

to the pendulum is not dependent on the distance between the slab and the target plate in the pendulum or on the type of pendulum.

Figure 7. View of the (horizontal) set-up of the experiments with the ballistic pendulum.

4.4 Determination of the properties of the particle stream

The data for the mass distribution have already been discussed in (Amelsfort and Weerheijm, 1987). The present report suffices with Table 7, which gives a review of the data obtained and the formulae derived from these data.

For measuring the velocity of the particle stream itself in the

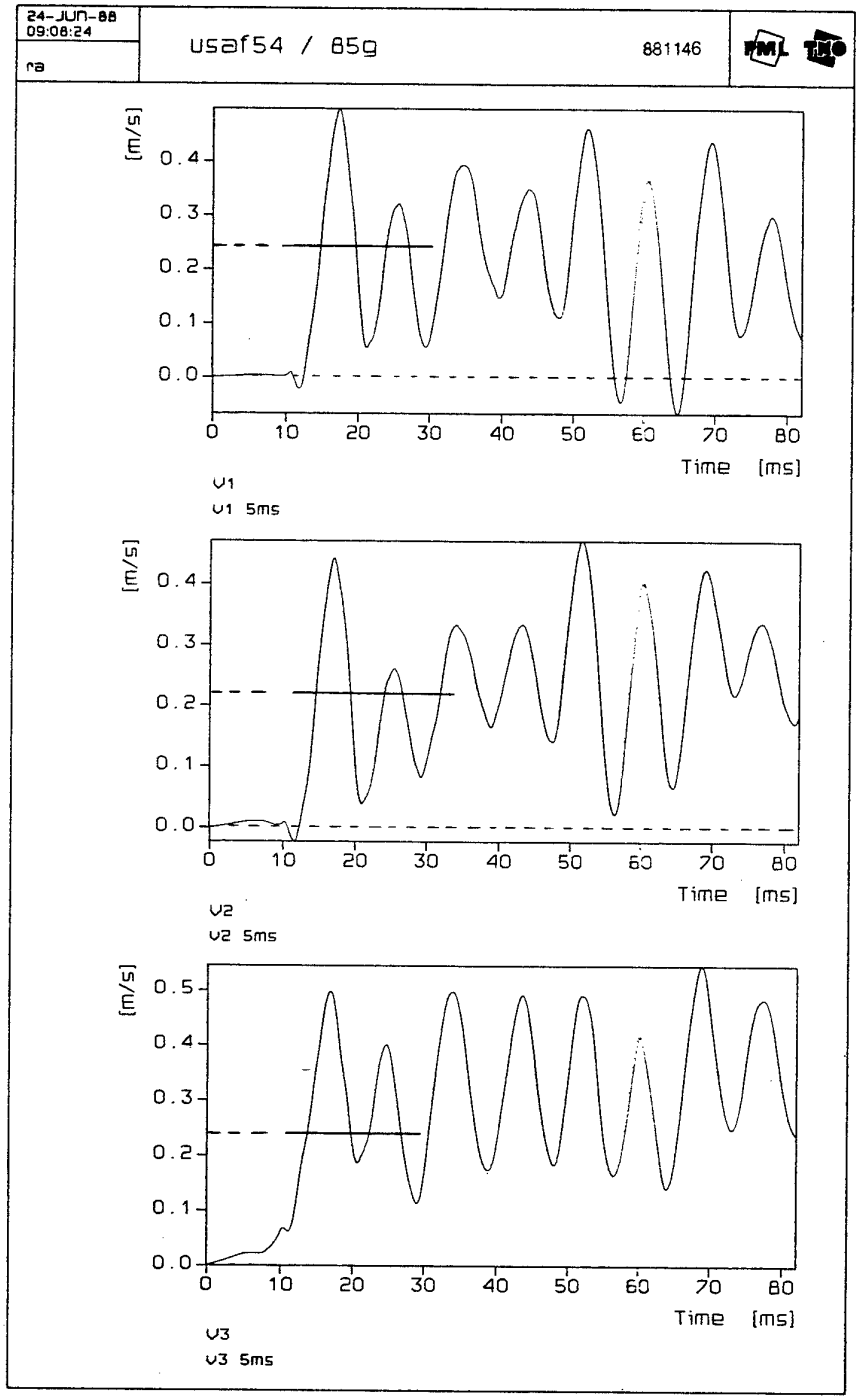

Figure 8. Resulting signal of the acceleration transducers after filtering, offset correction, integration and drift correction.

Calculated impulse transmitted to the pendulum Table 6.

Charge (g)	Exp. no.	I_{tf} (kgm/s)	I_{ta} (kgm/s)	I_{tp} (kgm/s)
50	22	47	25-42	55
	43	89	57-63	-
	44	47	37-42	-
	49	57	31-37	68
	52	52	47-63	57
	53	52	37-52	52
	58	42	31-42	52
	59	52	31-37	52
70	20	104	77-80	92
	23	72	89-94	85
85	19	112	104-109	117
	24	114	117-119	112
	45	99	84-104	-
	46	-	99-115	-
	50	84	52-63	73
	54	115	110-131	99
	55	104	115-136	99
	60	125	73-89	99
	61	125	63-78	104
170	21	226	184-211	206
	25	174	194-194	196
	47	193	214-235	-
	48	209	219-230	188
	51	146	115-141	-
	56	214	209-235	175
	57	219	240-256	188
	62	198	-	214
	63	198	198-224	183
	64	204	188-209	198

Concrete mass and particle size distribution Table 7.

Charge (g)	Exp no.	Total mass (g)	Mass with particle size: > 4 mm (g)	< 1 mm (g)	> 4 mm (%)	< 1 mm (%)
20	4	1332	679	306	51	23
40	3	2387	955	716	40	30
50	2	2829	1047	934	37	33
70	17	3512	1405	1159	40	33
	18	3448	1345	1172	39	34
75	1	3512	1299	1264	37	36
85	13	4415	1898	1369	43	31
	16	4181	1505	1547	36	37
120	01	4214	-	1475	-	35
	02	3794	1669	1328	44	35
122	03	3202	1505	833	47	26
170	14	4261	1491	1704	35	40
	15	4005	1242	1762	31	44

Derived formulae:

mass with particle size greater than 1 mm diameter:

$$P_{g1} = 45.20 * Q^{-0.15} \ (\%) \qquad (6)$$

mass with particle size greater than 4 mm diameter:

$$P_{g4} = 29.70 * Q^{-0.10} \ (\%) \qquad (7)$$

mass with particle size smaller than 1 mm diameter:

$$P_{l1} = 53.37 * Q^{0.175} = 100 - P_{g1} \ (\%) \qquad (8)$$

experiments a film technique appears to be the easiest way (Amelsfort and Weerheijm, 1987). When studying the films it appeared to be important whether the contact charge was placed just over the reinforcement or not. When the charge is placed over the reinforcement, the particle stream divides into two particle streams, while the divergence remains very small. When the charge is placed next to the reinforcement the particle stream remains intact, the divergence is negligible and the velocity is obviously higher. For the first metre of the trajectory of the concrete particles the impulse transferred to the target plate is not dependent on the distance (see paragraph 4.3). This means that for the calculation of the impulse by means of the product of data experimentally obtained for mass and velocity, average values for the velocity (tip velocity of the particle stream) and the total mass can be regarded as sufficient for a reliable value for the impulse. A review of these velocities, together with the width of the particle stream, is given in Table 8.
Examples of the particle stream for both cases, contact charge over and next to the reinforcement, are given in Figures 9 and 10.

For examining the behaviour of the concrete itself with respect to the process of cracking and spalling, an extra experimental programme has been set up. The main purpose of this programme was to get information about the propagation velocities of various stress levels in concrete. With this information the moment of interaction of the reflected precursor and the crushed zone can be determined. This includes that the time at which the mechanism of the particle stream is initiated, is also known. For this reason optical fibres were used to measure the response of concrete due to dynamic load (Dongen, 1988). The light transmission through the fibre related to the deformation of the fibre. If this relation is known and calibrated, the deformation of the fibre and the surrounding material, the concrete, can be deter-

Average velocity and width of the concrete particle stream. Table 8.

Charge (g)	Exp no.	Position charge with regard to reinforcement	Average velocity (m/s)	Width (mm)
50	28	over	120	200
	31	next to	170	250
	34	next to	160	220
	39	next to	155	220
70	35	next to	190	350
	40	next to	215	350
85	29	over	170	400
	32	next to	235	350
	36	next to	225	300
	41	next to	210	300
170	30	over	275	550
	33	next to	350	550
	38	next to	325	450

mined by measuring this light transmission. This method, which succeeded partly, is described in the Appendix. Numerical data for the propagation velocity cannot be given because of the disturbing influence of the light flash of the explosion in the final tests. For the same reason and due to the lack of knowledge of the relation mentioned before, numerical data for the stress levels cannot be given either.

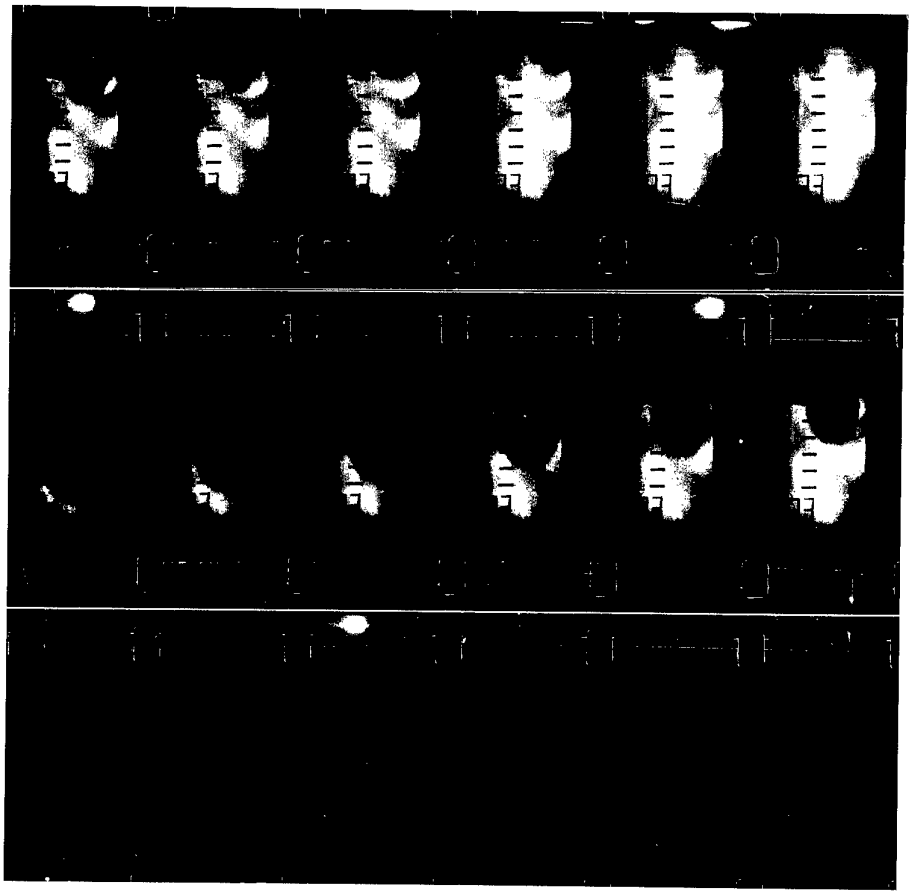

Figure 9. The formation of the concrete particle stream when the the contact charge is placed next to the reinforcement. (charge is 170 g)

5. DISCUSSION OF RESULTS

The experiments confirm the theory of a critical charge when a concrete slab is loaded with a contact charge, as described in (Weerheijm et al., 1984). Several phenomena can be observed for this critical charge, being 85 g of 80 % PETN for a 60-mm-thick concrete slab (Amelsfort and Weerheijm, 1987):

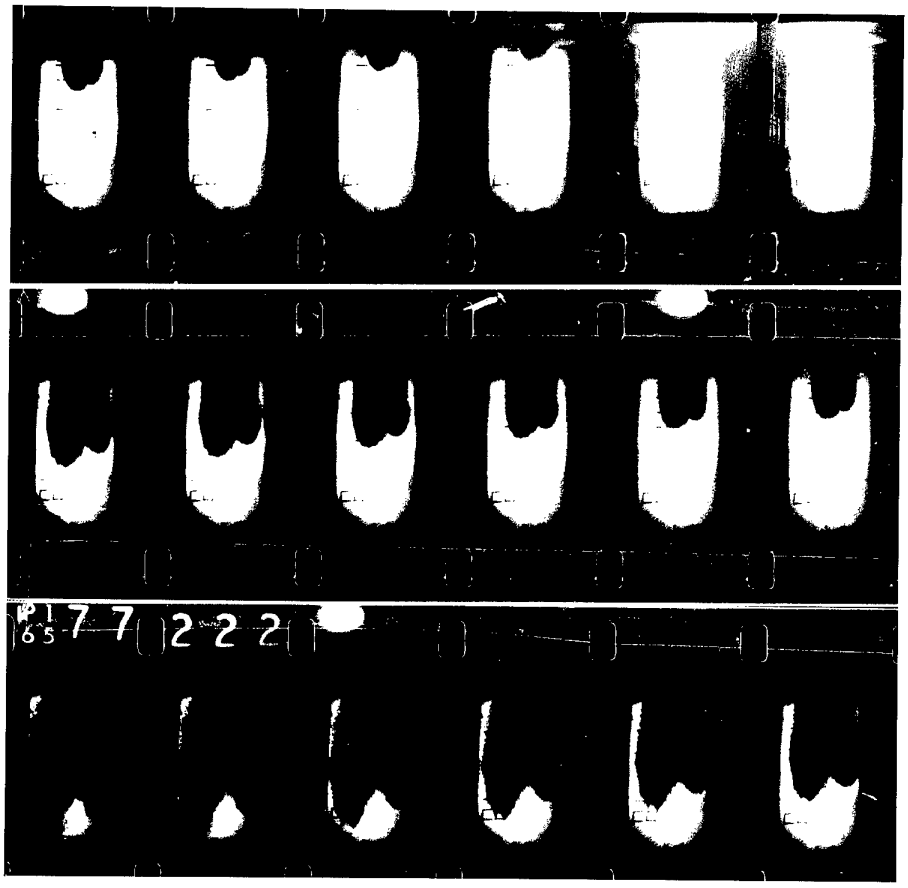

Figure 10. The formation of the concrete particle stream when the the contact charge is placed over the reinforcement. (charge is 170 g)

- The crater dimensions give a point of inflection at the critical charge.
- The concrete mass retrieved after the experiments has a maximum at the critical charge. Since the crater dimensions increase with increasing charge, the volume and the mass should increase too. A maximum in the retrieved mass means that the amount of dust which cannot be caught, increases with increasing charge.
- The retrieved concrete mass with particle size greater than 1 mm diameter has a maximum at the critical charge, while the retrieved mass with particle size less than 1 mm increases with increasing charge.

- The percentage of retrieved mass particles with particle size greater than 1 mm diameter decreases, and with particle size less than 1 mm diameter increases, with increasing charge.

These results do justify the conclusion that other phenomena occur for contact charges above the critical charge. For 80 % PETN the critical diameter d_c equals:

$$d_c = 13.4 * Q^{1/3} \quad (mm) \qquad (9)$$

with the charge Q in grams. When comparing the load performed by the particles originating from the crater at the back of the slab and the (small) particles ejected through the hole the following considerations can be made. Assuming the crater diameter d_b is double the hole diameter d (Table 4), the volume, and thus the masses of the particles of both origins differ about a factor 2 in favour of the crater particles, if geometrical and material damping are neglected. The maximum velocity of these particles can be calculated with $u = 2.f_c / \rho .c$. This results in u = 65 m/s when f_c is about ten times the static compression strength, ρ = 2200 kg/m^3 and c = 3500 m/s. Table 8 shows velocities of the particle stream of at least 200 m/s. Because of a factor of about 3 between these velocities, the difference between impulses in both cases is still a factor 2/3 against the crater particles. The durations of both loads determined by the quotient of half the slab thickness and the particle velocities also give a minimum factor of 3. The ratio of the squares of crater and hole equals a factor 4, owing to the double diameter. The average load performed by both types of loading can be calculated by dividing the impulses by the duration and the surface areas. This results in a factor 18 in favour of the particles ejected through the hole. So, when neglecting damping and using minimum particle velocities, the force of the load caused by the particle stream ejected through the hole is about 18 times the

force of the load caused by the spall particles. This means that for charges above the critical charge, the dominant force on following slabs is formed by the mass stream of small particles ejected through the hole that is punched in the slab, in accordance with the conclusions mentioned before (Weerheijm et al., 1984, Amelsfort and Weerheijm, 1987). For the mass M (in g), involved in this dominant force, a good estimate is given by:

$$M = \pi/4 * d^2 * (1/2\ h) * \rho * 10^{-6} \qquad (10)$$

with the hole diameter d and the slab thickness h (Figure 5) in mm and the concrete density ρ in kg/m^3. This mass M corresponds with the experimentally retrieved mass with particle size less than 1 mm diameter. A data fit for the average velocity V from the results as given in Table 8, results in:

$$V = 16.25 * Q^{0.587} \quad (m/s) \qquad (11)$$

with the charge Q in g. Here, V is the velocity in case the charge is positioned next to the reinforcement of the concrete. If the charge is situated just over the reinforcement, this velocity has a 15 to 25 % lower value. Multiplication of (10) and (11) gives an estimate of the supplied impulse I_s, by assuming the particle stream as a massive block with mass M and with an average velocity V. An expression for I_s (in kgm/s) can be found by substituting the hole diameter (4) in (10) and multiplying (10) and (11):

$$I_s = 6.093 * h * \rho * Q^{1.307} * 10^{-6} \qquad (12)$$

with the slab thickness h in mm, the concrete density ρ in kg/m^3 and the charge Q in g. This impulse is an ideal impulse while the

particle stream delivers a non-ideal impulse. This equation gives values for the supplied impulse of 133.6, 207.5, 267.4 and 661.6 kgm/s respectively for charges of 50, 70, 85 and 170 g (with h = 60 mm, ρ = 2200 kg/m^3). When these values of the impulse I_s are compared with the values of the impulse I_t transmitted to the pendulum (see 4.3) it appears that a part of the impulse is dissipated during the acceleration of the pendulum. In Table 9 the results of the comparison are reviewed.
The result of substituting the above - mentioned charges in the formula given in (Amelsfort and Weerheijm, 1987)

$$I_t^a = .777 * Q^{1.1} \qquad \text{(kgm/s)} \qquad (13)$$

yields 57, 83, 103 and 221 kgm/s respectively. Relation (13), which has been derived from the first tests, still appears to be applicable, as shown by the corresponding values in Table 9.

Review of values experimentally obtained
for the supplied and transmitted impulse. Table 9.

Charge (g)	Supplied impulse I_s(kgm/s)	Transmitted impulse I_t(kgm/s)	Quotient $\frac{I_s}{I_t}$
50	135	50	2.7
70	210	85	2.5
85	270	110	2.5
170	660	220	3.0

The quotient I_s / I_t is a measure for the loss of impulse during impact of the concrete particle stream onto the target plate in the pendulum. This loss is mainly caused by the non-ideality of the impulse delivered to the pendulum. The target load is not a solid mass with one velocity which hits the target plate, but a lot of (small) particles, each with its own velocity hitting the target plate at different times. Although the load of the pendulum is not ideal, the movement of the pendulum is like the movement of a mathematical pendulum, as already concluded in (Amelsfort and Weerheijm, 1987).

Now two ways of calculating the stress level of the particle stream are given, one following the theory of (Pahl, 1979) and one using the Crawford equation (1).
The formulae for the total impulse I_s^p (in Ns) due to the detonation pressure as given in (Pahl, 1979) is as follows:

$$I_s^p = \{183 - \frac{191}{1.10 + (ab/r^2)^{1/2}}\} * W \qquad (14)$$

where W is the charge in N, and a, b and r are dimensions of the contact charge. For a hemisphere a = b = 2r with r the radius of the sphere. So, when considering a hemisphere, eq. (14) results in:

$$I_s^p = 1.2 * Q \qquad \text{(kgm/s)} \qquad (15)$$

with Q the charge weight in g. This formula gives values of 60, 84, 102 and 204 kgm/s respectively for the above mentioned charges. These values for the total supplied impulse correspond with our measured values for the transmitted impulse as given in Table 9.
The total load F_b^p due to the detonation pressure is (Pahl, 1979):

$$F_b^p = \pi * P_b * R^2 \qquad (16)$$

Here P_b is the dynamic strength (in Pa), and equals about ten times the static compression strength, and R is the radius of the assumed load surface (in m). This means F_b^p is the load (in N) caused by the elastic precursory wave. The formula for R (in m) given by Pahl is:

$$R = 10.1 * (\frac{Q}{f_c})^{1/3} \qquad (17)$$

with the charge Q in g and the static compression strength f_c in Pa. The values calculated for R varies from 0.12 to 0.19 m for charges from 50 to 170 g. When these values are compared with the measured diameters, it appears that R corresponds with the crater diameter at the back. Pahl evidently considers the load performed by the particles to originate from the crater. For a static compression strength of 25 MPa these formulae result in values for the total load of 12.7, 15.8, 18.1 and 28.6 MN for 50, 70, 85 and 170 g contact charges, respectively. The quotient of the total impulse I_s^p (15) and the total load F_b^p (16) gives the pressure duration time t_d for a block load. On account of the assumption of a minimum value for the dynamic strength (ten times the static strength) and application of the crater diameter at the back ($I_s^p = I_t$), the pressure duration times resulting from these calculations are lower limits. In doing so, the values found for t_d in this way are 4.7, 5.3, 5.6 and 7.1 microseconds.

When using these duration times in combination with the values of the supplied impulse (I_s) from Table 9 and those of the hole diameter from Table 4, the loading can be calculated. For a block load assumption the resulting stress levels, as shown in Table 10, are of the order of 2 to 3 GPa, which is about 80 up to 100 times the static compression strength (25 - 30 MPa). This is an upper limit for the load supplied from the back of the concrete slab because the values for the duration time t_d are underestimated.

Calculated upper limit of the load performed by the particle stream. Values for I_s and d have been taken from Tables 4 and 9. Values of t_d have been calculated following (Pahl, 1979). Table 10.

Charge (g)	I_s (kgm/s)	t_d (s)	d (m)	$\pi/4.d^2$ A (m^2)	$\frac{I_s}{t_d}$ F (N)	F/A P_p (Pa)
50	135	$4.7*10^{-6}$	0.131	0.013	$29*10^6$	$2.2*10^9$
70	210	5.3	0.142	0.016	40	2.5
85	270	5.6	0.157	0.019	48	2.5
170	660	7.1	0.199	0.031	93	3.0

By considering the quotient of half the thickness of the slab (30 mm) and particle velocity (Table 8), maximum values for the duration times can be calculated, resulting in minimum values for the load P_p. In this case stress levels of 55 to 235 MPa are obtained, which is about 2 to 10 times the static compression strength (Table 11).

Crushed concrete has some similarity to loose dry sand. With the use of equation (1) and the properties of concrete (ρ = 2200 kg/m^3 and c = 3500 m/s), respectively loose dry sand (ρ = 1500 kg/m^3 and c = 500 m/s), values for the load P_p can be calculated for both materials, as shown in Table 12. Concerning the quotient of the acoustic impedances (ρ .c), of concrete and loose dry sand, which equals a factor 10, the same factor is found for the load F for both materials. This means that the 'concrete' value for P, as given in Table 12, is an overestimated one, because of the

Calculation of the lower limit for the load exerted by the particle stream. Values for I_s and A taken from Table 10. Values for u the same as in Table 8. Table 11.

Charge (g)	I_s (kgm/s)	u (m/s)	t_d (s)	A (m^2)	$\frac{I_s}{t_d}$ (N)	P_p (Pa)
50	135	160	$1.9*10^{-4}$	0.013	$0.7*10^6$	$55*10^6$
70	210	200	1.5	0.016	1.4	88
85	270	225	1.3	0.019	2.1	110
170	660	340	0.9	0.031	7.3	236

decreasing values for the density and wave velocity, when the concrete has been crushed. The 'sand' value for P on the other hand will probably be an underestimated one.

Finally, a summary of the different ways for estimating the load level at the back of the concrete slab will be given. Division of experimentally determined I_s values and underestimated t_d values (Pahl, 1979) gives an upper limit of 2200 to 3000 MPa for the load level (Table 10). Making use of overestimated t_d values (from measured particle velocity and slab thickness) results in a lower limit of 55 to 235 MPa (Table 11). Calculations with the acoustic impedances of concrete and loose dry sand (Table 12) result in overestimated values of 1200 to 2600 MPa (concrete) and underestimated values of 120 to 260 MPa (sand). These results together with the knowledge of the static compression strength (25 to 30

MPa) indicate a stress level at the back of the concrete slab of 400 to 1000 MPa at critical charges.

Calculation of the load performed by particle streams of concrete (density ρ = 2200 kg/m^3, longitudinal wave velocity c = 3500 m/s) and loose dry sand (ρ = 1500 kg/m^3 and c = 500 m/s). The values of the particle velocities u have been taken from Table 8. Table 12.

Charge (g)	Concrete: u (m/s)	$P_p = u.\rho.c$ (Pa)	Loose dry sand: $P_p = u.\rho.c$ (Pa)
50	160	$1.2*10^9$	$0.12*10^9$
70	200	1.5	0.15
85	225	1.7	0.17
170	340	2.6	0.26

6. CONCLUSIONS

- A critical thickness does exist. When exceeding the corresponding critical load, other phenomena occur. The concrete particle stream consists of an increasing percentage of small particles of high energy.
- The assumption for the dynamic strength to be 8 to 10 times the static compression strength seems reasonable.
- The influence of the reinforcement of the concrete on the force of the particle stream is remarkable. When the charge is located just over the reinforcement, the velocity of the concrete

particles reduces by about 75 %. This means that a reinforcement with small meshes will reduce the threat of the load for subsequent slabs by 75 %.

- The divergence of the concrete particle stream is negligible, so the distance between two successive slabs has no influence for the first metre at least.
- The supplied impulse, calculated as the product of total particle mass and average particle velocity amounts to about 2.5 to 3 times the measured transmitted impulse. This can be explained by the non-ideality of the stream. The tail of the particle stream will contribute much less to the total impulse than the head of the stream.
- The use of a fibre technique for measuring the response of concrete to contact charges looks promising. However, some problems have to be solved first. Investigations into the experimental fibre technique should be continued.
- The main load at critical charges is formed by the concrete particles ejected through the punched hole. The stress level at the back of the slab is estimated to be about 400 to 1000 MPa.

7. AUTHENTICATION

Date: November 1988

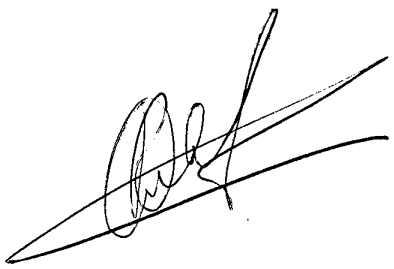

J. Weerheijm R.v.Amelsfort

8. REFERENCES

Pahl, H.
Obererdische und erdversenkte Schutzbauten fur Kriegshauptquartiere gegen die Wirkung konventioneller Waffen.
Bericht über das 100. Wehrtechnische Symposium Waffenwirkung und Schutzbauten, Mannheim, August 1979.

Weerheijm, J., Karthaus, W., Opschoor, G.
The failure mode of layered concrete constructions due to contact charges.
21st Dod Explosives Safety Seminar, August 1984.

Amelsfort, R.v., Weerheijm, J.
The failure mode of concrete slabs due to contact charges.
Progress Report No.1, 30 Sept. 1986 - 27 Febr. 1987.
PML 1987-IN18, Grant AFOSDR-86-0340 DEF

Amelsfort, R.v., Weerheijm, J.
The failure mode of concrete slabs due to contact charges.
Interim Scientific Report, Sept. 30th. 1986 - Sept. 29th. 1987.
PML 1987-C146, Grant AFOSDR-86-0340

Kolkert, W., Amelsfort, R.v.
Ballistic pendulum methodology to study armour / anti - armour interactions at oblique impact.
33rd. Conference Aeroballistic Range Association, 1982.

Kolkert, W., Amelsfort, R.v.
Study of armour / anti - armour interactions at oblique impact with a ballistic pendulum methodology.
7th International Symposium on Ballistics, 1983.

Dongen, P.v.
Optische fibers als druksensor in een betonplaat belast door een kontaktlading (in Dutch).
PML-1988 (in preparation).

APPENDIX

As part of the investigation into the response of concrete due to contact charges, an experimental programme has been set up to examine the possibilities of several measuring methods. Electronic methods appear to be unsuitable because of the electromagnetic pulse effect (EMP), caused by the explosion, unless special precautions are taken to minimize the EMP. This can probably be obtained efficiently by covering the explosive charge with an earthed aluminium foil.
A very promising method appears to be a method using optical fibres to register the material response under dynamic loading circumstances by measuring the light transmission of the fibres at different positions in the slab. This light transmission is related to the deformation of the fibre and thus to the surrounding material. When the relationship between the dynamic load and the light transmission as well as the influence of the geometry on the load to the light transmission are known, it will be possible to transform the measured light transmission into real pressure values. Without this knowledge it will still be possible to register the profile of the pressure wave and the propagation velocity. When the propagation velocities of the various stress levels in concrete are known, the moment of interaction between the reflected precursor and the crushed zone can be determined. With this information the time at which the mechanism of the particle stream is initiated can be determined. However, quantification of the stress levels requires calibration. Several types of fibre have been used in experiments, and the most suitable one for this type of problems appears to be a multimode step-index type fluorine polymer fibre (fabric: Mitsubishi CO., Ltd. Type Super ESKA SH-2001), especially developed for light transmission over short distances. With these fibres pressure measurements as a function of time are performed at different depths in the concrete, and the failure of concrete can be examined at different stages of the propagating pressure wave. Figure 11 gives a view of the theoretical response of the fibre

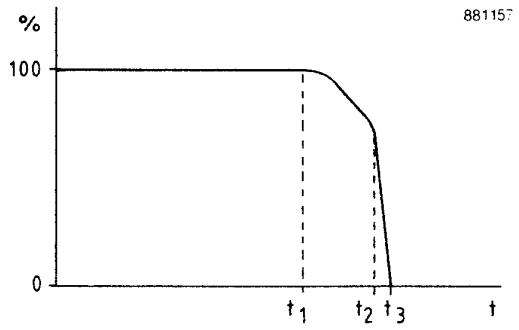

Figure 11. Theoretical response of a fibre to an explosive load:
t_1 = arrival of pressure wave (elastic)
t_2 = fracture of concrete (plastic)
t_3 = fibre completely intersected.

exposed to an explosive load. The elastic pressure wave (precursor) compresses the fibre, which results in a gradual decrease in light intensity (t_1). The plastic pressure wave fractures the fibre as a concequence of the deformation of the surrounding concrete, so no light will be transmitted any more (t_2). However, some light originating from the explosion may still be detected.
For the experiments 6 fibres at a distance of 10 mm from each other, are embedded in a concrete slab of 50 mm thickness, as shown in Figure 12. The coil shown in Figure 12 is meant to measure the EMP (which does not influence the light transmission). The fibres are placed below each other in one plain and below the contact charge in the centre of the slab. Each fibre is connected with a light source with constant light intensity. The light passing through the fibre is

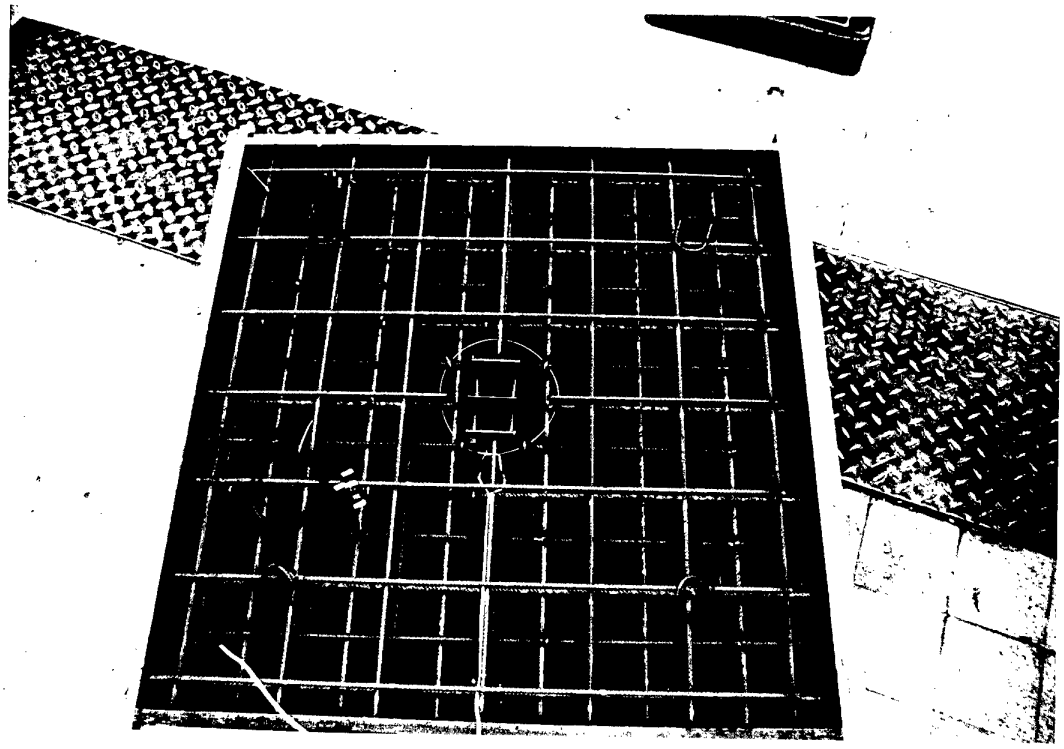

Figure 12. Fibres and coil before the bulk of the concrete.

finally converted into a voltage, with the aid of a light-voltage converter and a voltage-amplifier.

Several preliminary experiments have been performed, which proved that the method comes up to expectations. Figure 13 shows the results of one preliminary experiment. It can clearly be seen that the 6 successive fibres give a signal at 6 successive times.

The link with values for the magnitude of the deformations cannot be made at this moment, because of the absence of a relation between the fibre signal and the deformation of the fibre.

A second set of experiments, with the same geometry of the slab and the same type of fibres, has been performed. In this series a new problem arises concerning the duration of the light flash, which is of the same order of magnitude as the signal to be expected. This light flash causes an overload of the amplifier, which makes the signals

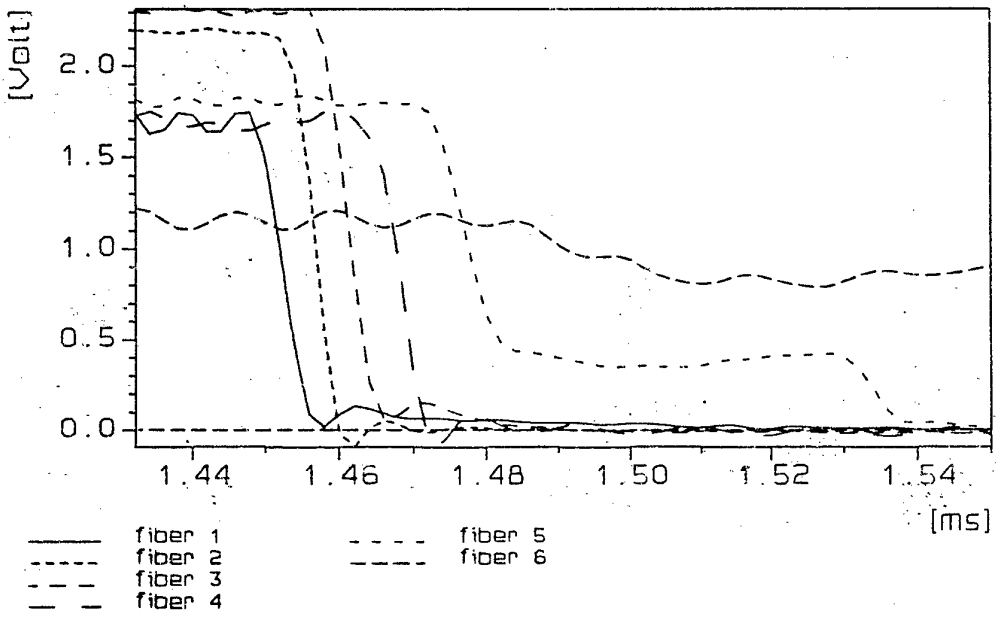

Figure 13. Result of a preliminary experiment, representing the response time in ms of six successive fibres at 10 mm of each other.

useless after this moment. A simple solution for this problem is to use thicker concrete slabs. An extra advantage of thicker plates is a greater accuracy of the measurements. The times at which changes in light intensities are measured can be used to determine the propagation velocity of the crushed area. A more detailed description of the experiments performed is given in (Dongen, 1988).